24th COBEM - 2017

24th ABCM International Congress of Mechanical Engineering
December 3-8, 2017, Curitiba, PR, Brazil

COBEM-2017-0359
UNCERTAINTY ANALYSIS ON STABILITY OF A RIGID ROTOR WITH HYDRODYNAMIC BEARINGS

Laís Bittencourt Visnadi
Hélio Fiori de Castro
School of Mechanical Engineering, University of Campinas - UNICAMP, Campinas, Brazil
lais.visnadi@fem.unicamp.br and heliofc@fem.unicamp.br

Abstract. *Uncertainties about project parameters may generate early failures in a system. This study investigates the influence of these uncertainties on the unstable vibration of a rigid rotor with hydrodynamic bearings, due to fluid induced instability.*
For rotors supported by cylindrical lubricated bearings, it is known that there is a threshold of instability on the rotation speed of the system. Considering variation on bearing parameters, that may be caused by manufacturing process or wear of components, and variation of oil viscosity that may occur due to temperature variations, the Monte Carlo method was used to evaluate the variation of these threshold.
Results show that points of transition may vary considerably. Considering the instable motion as an undesirable situation, since the increase of vibration can cause severe damage, it is possible to determine a maximum allowable rotation for a determined reliability for the rotor.

Keywords: *rotor, hydrodynamic bearing, uncertainty, stability*

1. INTRODUCTION

The rotor is a mechanism widely used on machines and its failure can cause severe damage. Consider its stability is required for a safe operation. However, the calculation of this stability depends on parameters that may vary randomly, so this point of transition from stable to unstable is also subject to vary. This variation may cause early failure if the point of transition is lower than the previously calculated.

Researches about this instability progressed in the 1920's, when Newkirk (1925) discovered this phenomenon. Bently (2001) states that this stability depends on the interaction of shaft, oil film and bearing. He showed that the phenomenon known as oil whirl depends on the shaft angular velocity and the phenomenon known as oil whip depends on mechanical variables, such as shaft mass and stiffness.

Didier et al. (2012) investigated the effects of uncertainties such as unbalance, bow and misalignments on the variability of the nonlinear response in rotor systems. Machado et al., (2015), investigated the bearing wear (which affects bearing clearance) influence on the dynamic response of a rotor-bearing system.

The objective of this paper is to investigate the influence of uncertainties in bearing parameters on the stability threshold of a rigid rotor with hydrodynamic bearings.

2. COMPUTATIONAL PROCEDURE

Figure 1 shows a scheme of a hydrodynamic bearing.

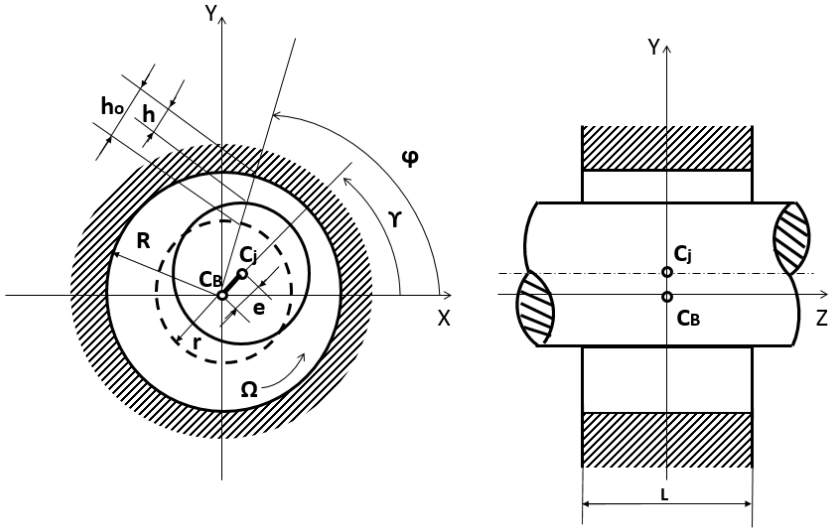

Figure 1. Scheme of a hydrodynamic bearing. Adapted from Krämer (1993)

C_B is the bearing center, C_J is the journal center. This points are coincident if the journal is unloaded. e is the journal eccentricity and, with the angle γ, they define the journal position. R is the bearing radius, L is the bearing length and r is the journal radius. h_o is the bearing clearance, also denoted by δ and defined by the difference between R and r (bearing clearance). The journal rotation is Ω.
For a moving journal with $e(t)$ and $\gamma(t)$:

$$h(\varphi,t) = h_o(\varphi) - e(t)\cos[\varphi - \gamma(t)] \tag{1}$$

It is assumed that:

1. The lubricant is incompressible, massless, Newtonian, adheres to bearing surfaces, its viscosity is constant in the whole of the oil-film and its pressure is constant in the radial direction;
2. The flow is laminar and is velocity in radial direction is neglected;
3. Velocity gradients in redial direction are large compared to velocities in tangential and axial directions;
4. The oil-film curvature is negligible and its thickness is small compared to the journal radius;
5. The bearing surfaces are stiff and smooth.

Then, the Reynolds Equation is valid:

$$\frac{1}{R^2}\frac{\partial}{\partial\varphi}\left(h^3\frac{\partial p}{\partial\varphi}\right) + h^3\frac{\partial^2 p}{\partial z^2} = 6\eta\left[\Omega\frac{\partial h_o}{\partial\varphi} + e(\Omega - 2\dot{\gamma})sin(\varphi-\gamma) - 2\dot{e}\cos(\varphi-\gamma)\right] \tag{2}$$

Sommerfeld (1904) developed the solution for this equation for long bearings.
Considering the bearing as short ($L/D \leq 0.5$), there is a complete solution for Reynolds Equation, proposed by Ocvirk (1952). In this case, the change in pressure along the circumferential direction is small in relation to pressure change in axial direction, so it is considered that $\partial p/\partial\varphi = 0$. It is possible, then, to integrate the Reynolds Equation and obtain a pressure function. Considering $dp/dz = 0$ for $z = 0$ and $p = 0$ for $z = \pm L/2$, it follows that:

$$p(\varphi,z,t) = \frac{3\eta}{h^3}[e(\Omega - 2\dot{\gamma})\sin(\varphi-\gamma) - 2\dot{e}\cos(\varphi-\gamma)]\left(z^2 - \frac{L^2}{4}\right) \tag{3}$$

Integrating over z, one obtains the oil-film force per unit length in the circumferential direction:

$$q(\varphi,t) = \frac{\eta L^3\Omega}{2\delta^2}\frac{\varepsilon\left(\frac{2\dot{\gamma}}{\Omega} - 1\right)\sin(\varphi-\gamma) + \frac{2\dot{\varepsilon}}{\Omega}\cos(\varphi-\gamma)}{[1-\varepsilon\cos(\varphi-\gamma)]^3} \tag{4}$$

Where ε is the eccentricity ratio, given by

$$\varepsilon = \frac{e}{\delta} \tag{5}$$

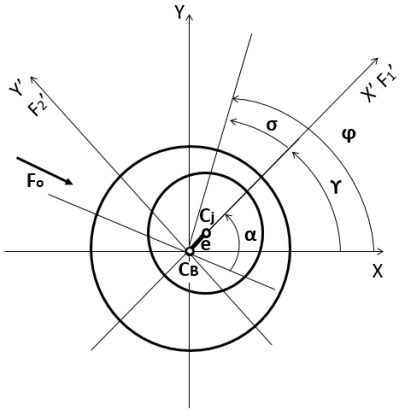

Figure 2. Components of oil-film force on a hydrodynamic bearing. Adapted from Krämer (1993)

The components of the oil-film force, that is of the journal force in the X', Y'- system are

$$F_1' = \int_{\pi}^{2\pi} q(\sigma, t) cos\sigma \; R \; d\sigma = F_\eta f_1(\varepsilon, \dot{\varepsilon}, \dot{\gamma}) \tag{6}$$

$$F_2' = \int_{\pi}^{2\pi} q(\sigma, t) sin\sigma \; R \; d\sigma = F_\eta f_2(\varepsilon, \dot{\varepsilon}, \dot{\gamma}) \tag{7}$$

With $\sigma = \varphi - \gamma$

$$F_\eta = \frac{\eta L^3 \Omega R}{2\delta^2} \tag{8}$$

$$f_1(\varepsilon, \dot{\varepsilon}, \dot{\gamma}) = \left(1 - \frac{2\dot{\gamma}}{\Omega}\right) \frac{2\varepsilon^2}{(1-\varepsilon^2)^2} + \pi \frac{\dot{\varepsilon}}{\Omega} \frac{1 + 2\varepsilon^2}{(1-\varepsilon^2)^{5/2}} \tag{9}$$

$$f_2(\varepsilon, \dot{\varepsilon}, \dot{\gamma}) = -\frac{\pi}{2}\left(1 - \frac{2\dot{\gamma}}{\Omega}\right) \frac{\varepsilon}{(1-\varepsilon^2)^{\frac{3}{2}}} - \frac{\dot{\varepsilon}}{\Omega} \frac{4\varepsilon}{(1-\varepsilon^2)^2} \tag{10}$$

In the X,Y-system, the force components are:

$$F_1 = F_1' cos\gamma - F_2' sin\gamma \tag{11}$$

$$F_2 = F_1' sin\gamma - F_2' cos\gamma \tag{12}$$

According to Krämer (1993), for a horizontally supported shaft with static loading F_o, $F_1 = 0$ and $F_2 = -F_o$.
It is possible then to obtain a relation between F_o and F_η, which is the friction force on the journal:

$$\frac{F_o}{F_\eta} = \frac{\pi}{2} \frac{\varepsilon}{(1-\varepsilon^2)^2} \sqrt{1 - \varepsilon^2 + \left(\frac{\pi}{4}\varepsilon\right)^2} \tag{13}$$

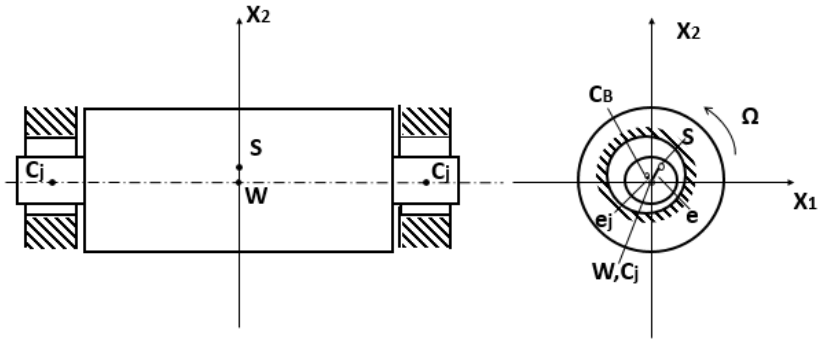

Figure 3. Scheme of a rigid rotor with hydrodynamic bearing. Adapted from Krämer (1993)

The shaft on Fig. 3 is rotating at angular velocity Ω and is loaded in its central plane with a static force $2F_0$, which is the dead weight $G = mg$. So, it is possible to relate the angular velocity of the shaft Ω and the eccentricity ratio ε, generating a startup curve of this ratio.
With the differentials of F_1 and F_2 with respect to x_1 and x_2, it is possible to obtain the stiffness and damping coefficients:

$$\frac{\partial F_i}{\partial x_k} = \frac{\partial F_i}{\partial \varepsilon}\frac{\partial \varepsilon}{\partial x_k} + \frac{\partial F_i}{\partial \gamma}\frac{\partial \gamma}{\partial x_k} \tag{14}$$

$$\frac{\partial F_i}{\partial \dot{x}_k} = \frac{\partial F_i}{\partial \dot{\varepsilon}}\frac{\partial \dot{\varepsilon}}{\partial \dot{x}_k} + \frac{\partial F_i}{\partial \dot{\gamma}}\frac{\partial \dot{\gamma}}{\partial \dot{x}_k} \tag{15}$$

Where i=1,2 and k=1,2.

$$\frac{\partial F_i}{\partial x_k} = k_{ik} = \gamma_{ik}\frac{F_o}{\delta} \tag{16}$$

$$\frac{\partial F_i}{\partial \dot{x}_k} = d_{ik} = \beta_{ik}\frac{F_o}{\delta\Omega} \tag{17}$$

Where

$$\gamma_{11} = [2\pi^2 + (16 - \pi^2)\varepsilon^2]A(\varepsilon) \tag{18}$$

$$\gamma_{12} = \frac{\pi}{4}\frac{\pi^2 - 2\pi^2\varepsilon^2 - (16 - \pi^2)\varepsilon^4}{\varepsilon(1 - \varepsilon^2)^{1/2}}A(\varepsilon) \tag{19}$$

$$\gamma_{21} = -\frac{\pi}{4}\frac{\pi^2 + (32 + \pi^2)\varepsilon^2 + (32 - 2\pi^2)\varepsilon^4}{\varepsilon(1 - \varepsilon^2)^{1/2}}A(\varepsilon) \tag{20}$$

$$\gamma_{22} = \frac{\pi^2 + (32 + \pi^2)\varepsilon^2 + (32 - 2\pi^2)\varepsilon^4}{1 - \varepsilon^2}A(\varepsilon) \tag{21}$$

$$\beta_{11} = \frac{\pi}{2}\frac{(1 - \varepsilon^2)^{1/2}}{\varepsilon}[\pi^2 + (2\pi^2 - 16)\varepsilon^2]A(\varepsilon) \tag{22}$$

$$\beta_{12} = \beta_{21} = -[2\pi^2 + (4\pi^2 - 32)\varepsilon^2]A(\varepsilon) \tag{23}$$

$$\beta_{22} = \frac{\pi}{2}\frac{\pi^2 + (48 - 2\pi^2)\varepsilon^2 + \pi^2\varepsilon^4}{\varepsilon(1 - \varepsilon^2)^{1/2}}A(\varepsilon) \tag{24}$$

$$A(\varepsilon) = \frac{4}{[\pi^2 + (16 - \pi^2)\varepsilon^2]^{3/2}} \tag{25}$$

The equations of motion for a rigid rotor, considering free vibration, are explicit in Equation (26):

$$\begin{aligned} m\ddot{x}_1 + 2(d_{11}\dot{x}_1 + d_{12}\dot{x}_2 + k_{11}x_1 + k_{12}x_2) = 0 \\ m\ddot{x}_2 + 2(d_{21}\dot{x}_1 + d_{22}\dot{x}_2 + k_{21}x_1 + k_{22}x_2) = 0 \end{aligned} \tag{26}$$

Their solutions are $x_1 = \varphi_1 e^{\lambda t}$ and $x_2 = \varphi_2 e^{\lambda t}$. Substituting these in the equations of motion, it is possible to find its eigenvalues. They are usually complex conjugate. The real part describes the growth of vibration. So, if this part is negative, the vibration of the system will decrease with time, so the system is stable. On the contrary, if the real part is positive, the vibration of the system increases with time, so it is unstable. Thus, if the real part is equal to zero, it is the threshold of instability. The imaginary part describes the frequency of the movement. At the stability borderline, $\lambda = 0$. It is possible, as shown by Krämer (1993), to obtain the natural frequency at the stability borderline:

$$\Omega_{th} = \sqrt{\frac{2.F_o.A_1.A_2.A_3}{\delta.m.(A_1^2 - A_1.A_3.A_4 + A_0A_3^2)}} \tag{27}$$

Where

$$A_0 = \gamma_{11}\gamma_{22} - \gamma_{12}\gamma_{21} \tag{28}$$

$$A_1 = \gamma_{11}\beta_{22} - \gamma_{12}\beta_{21} + \gamma_{22}\beta_{11} - \gamma_{21}\beta_{12} \tag{29}$$

$$A_2 = \beta_{11}\beta_{22} - \beta_{12}\beta_{21} \tag{30}$$

$$A_3 = \beta_{11} + \beta_{22} \tag{31}$$

$$A_4 = \gamma_{11} + \gamma_{22} \tag{32}$$

The natural frequency at the stability borderline is a function of the eccentricity ratio ε, which is a function of the angular velocity of rotation of the shaft Ω.
There are uncertainties about the rotor dimensions, such as the bearing clearance δ, the bearing radius R, and the bearing length L (arising from the manufacturing process or even from wear) and about the oil viscosity η (due to temperature variations). To represent these variations, samples of these variables were generated, from a gamma distribution, and the Monte Carlo method, as described by Sampaio et al (2012) was used to generate the startup curves and the borderline curves.
For a given system, there is a constant C_s which is defined by:

$$C_s = \sqrt{g}\frac{m\delta^{2,5}}{\eta R L^3} \tag{33}$$

This constant defines the behaviour of the start-up curves, as shown in Fig. 4:

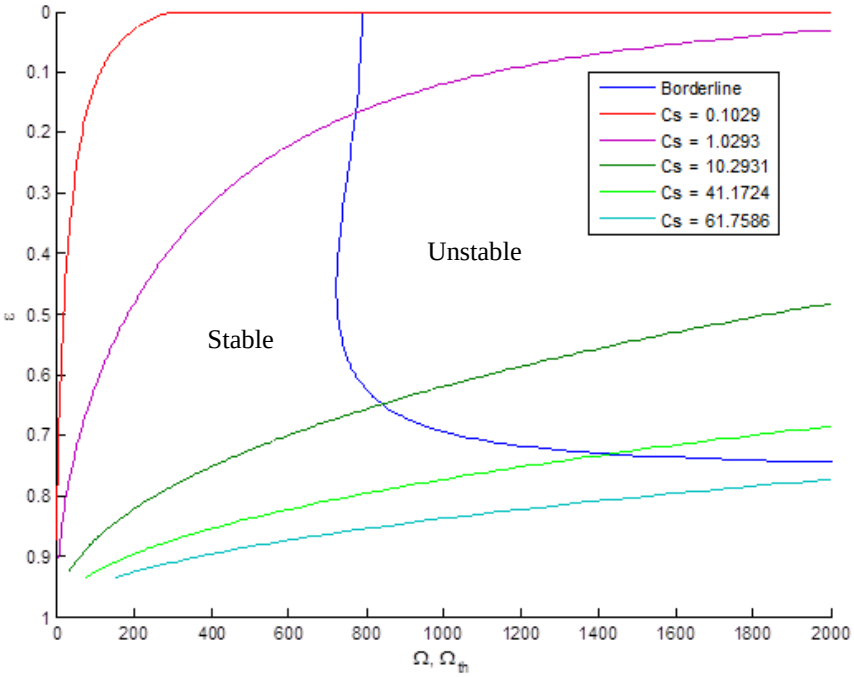

Figure 4. Influence of constant C_s on the start-up curves.

It is possible to notice that if C_s is under the value of 10, the rotor is considered to be "light" and the threshold of stability is quite constant, around 700rad/s. If its value is from 10 to 50 (approximately), the rotor is considered "heavy" and the threshold varies. If its value overcomes 50 (approximately), the system no longer becomes unstable.
This paper investigated the variations for both light and heavy rotors, and the parameter varied for this purpose was the disc mass (the values used were 10kg, 100kg and 200kg).
The other parameters were varied according to a gamma distribution. The mean and the standard variations of these values are shown in Tab. 1:

Table 1. Mean values and standard deviation for each variable

Variable	Mean Value	Standard Deviation
δ (bearing clearance) [μm]	120	5
η (oil viscosity) [Pa.s]	0.03	0.002
R (bearing radius) [mm]	20	0.05
L (bearing length) [mm]	20	0.05

3. RESULTS

Figure 5 shows de probability density function of the transition points for a given rotor, for 1,000, 5,000, 10,000 and 15,000 points in each gamma distribution for each variable. It is possible to notice that the results provide the same *pdf*, so it is known that the Monte Carlo simulation may be executed for 1,000 points without any loss. This work was done with 3,000 since the computational cost wasn't high and the results would be satisfactory.

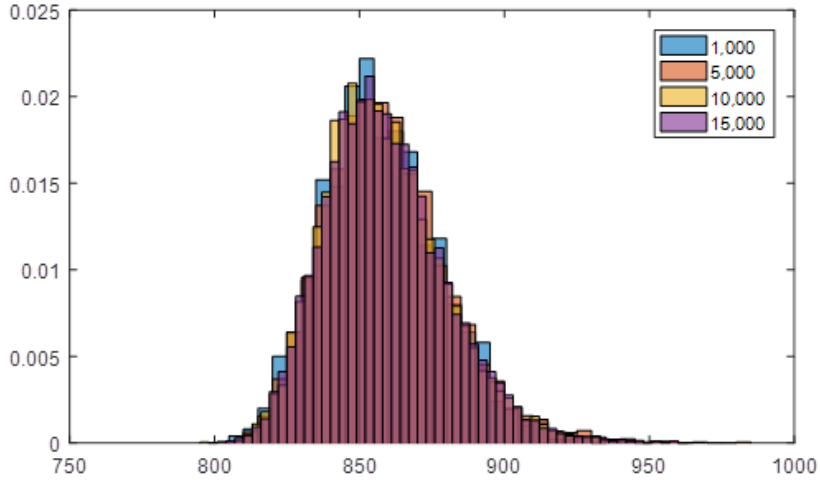

Figure 5. Probability density function of angular velocities of transition for a given rotor, varying the number of elements in each gamma distribution for each variable.

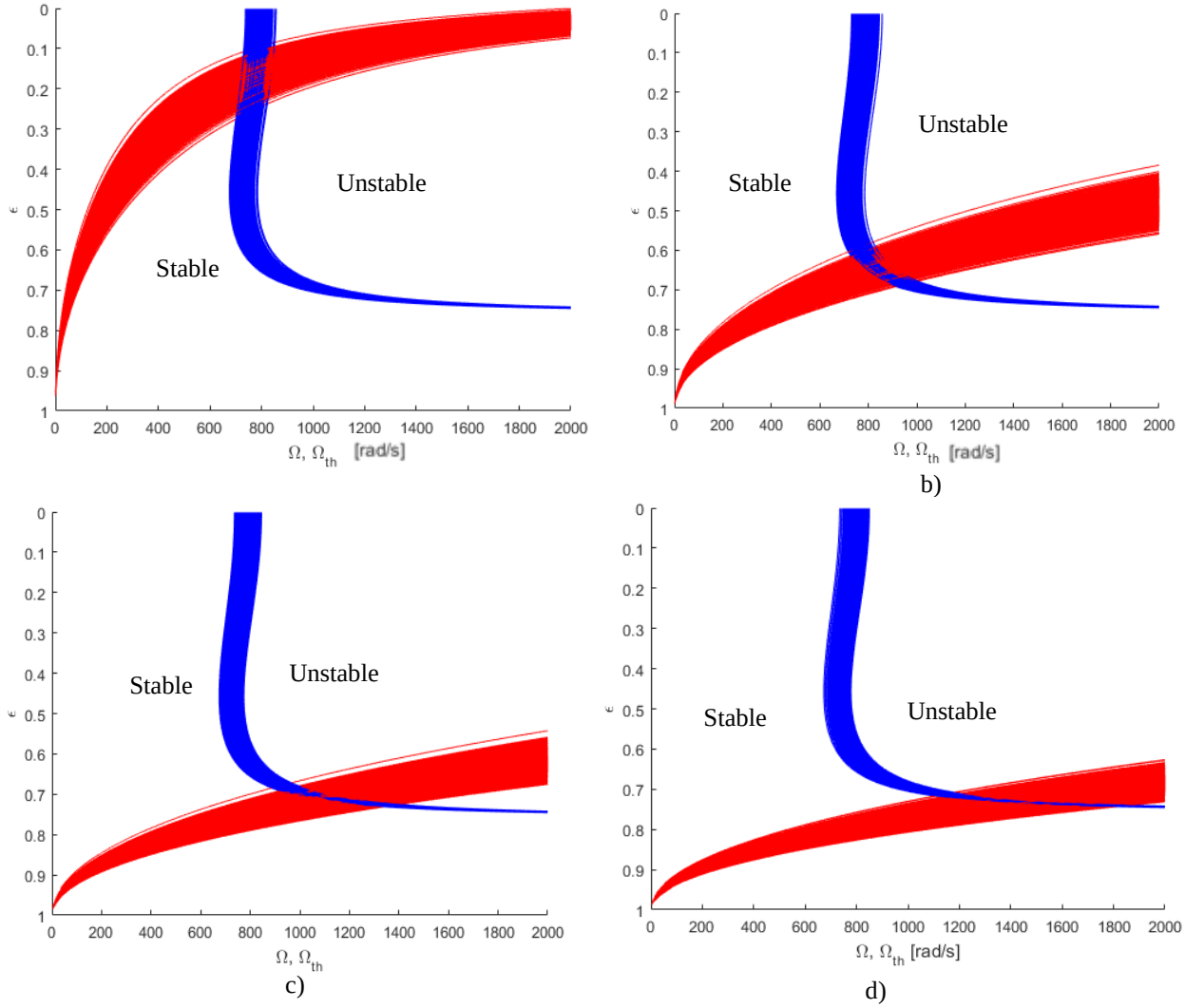

Figure 6. Start-up curves (red) and borderline curves (blue) for a)“light” rotor (m=10kg); b) “heavy” rotor (m=100kg); c) “heavy” rotor (m=200kg); d) “heavy” rotor (m=300kg)

Figure 6 indicates that for a “light” rotor, the threshold occurs in a low rotation compared to “heavy” rotors. It is also possible to notice that, the heavier the rotor, the more the threshold varies, so this limit of stability is more uncertain.

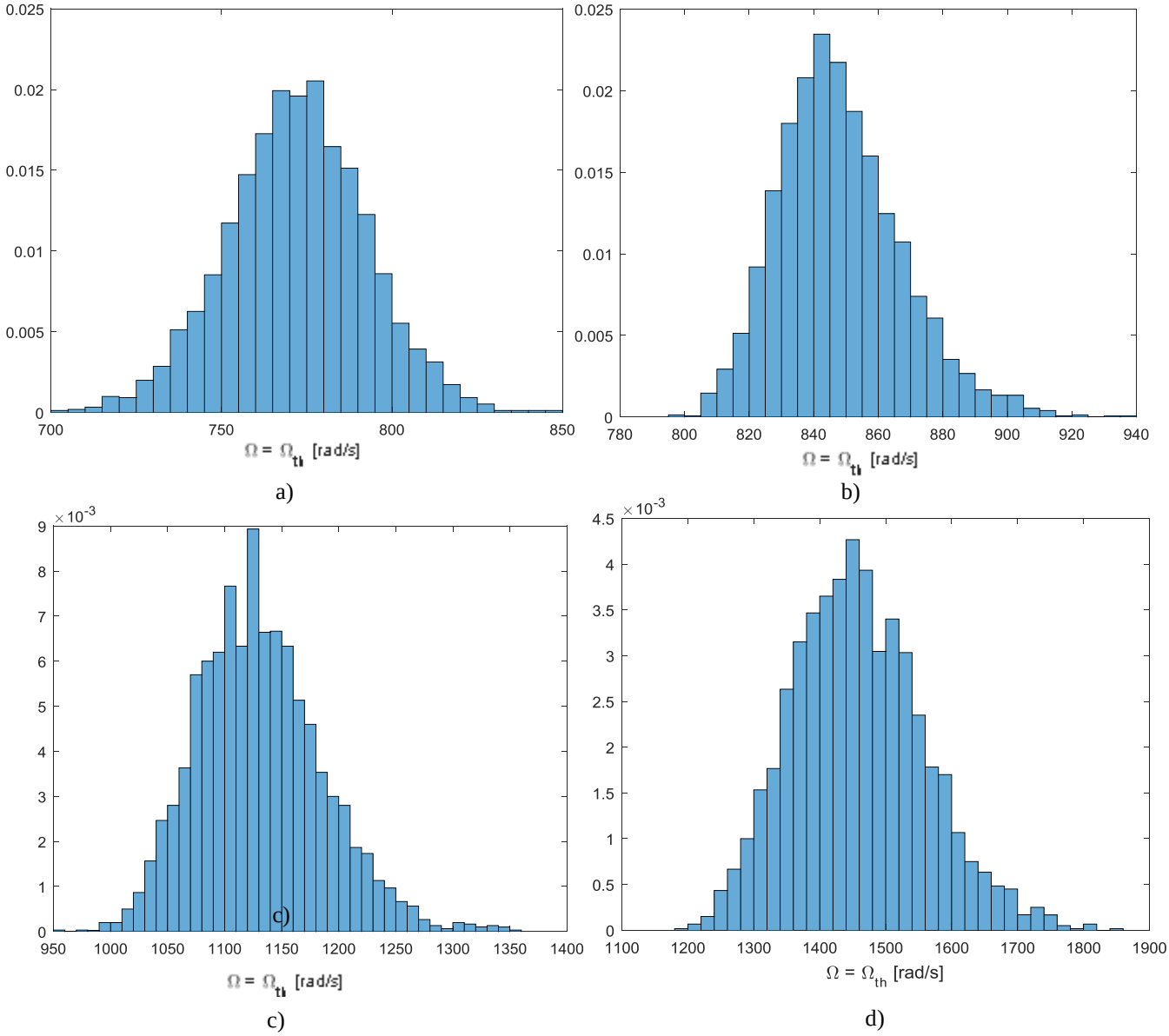

Figure 7. Probability density function of angular velocities of transition for a)“light” rotor (m=10kg); b) “heavy” rotor (m=100kg); c) “heavy” rotor (m=200kg); d) “heavy” rotor (m=300kg))

Figures 7 show the probability density function of the angular velocity of transition from stable to unstable for the related systems. Considering the transition to unstable as a failure, since excessive vibration leads to early failures in mechanical systems, it is possible to obtain a limit for the angular velocity of the rotor according to the desired reliability;

Consider Fig. 7a): if a 99% reliability is satisfactory, an angular velocity up to 740 rad/s is allowable. However, if a maximum reliability is desired, it is recommended not to overcome 700 rad/s. The skewness of this distribution is -0.0266, so it is almost symmetric, with a slight tendency to the right.

Analogously, in Fig. 7b) it is possible to notice that for a 99% reliability, the limit is around 820 rad/s and for maximum reliability it should be under 780 rad/s. The skewness of this distribution is 0.6015, so it is non-symmetric with a tendency to the left.

Analyzing Fig. 7c), for a 99% reliability, the limit is around 1040 rad/s and for maximum reliability it should be under 950 rad/s. The skewness of this distribution is 0.4740, so it is also non-symmetric with a tendency to the left.

Lastly, observing Fig. 7d), for a 99% reliability, the limit is around 1320 rad/s and for maximum reliability it should be under 1200 rad/s. The skewness of this distribution is 0.3518, so it is also non-symmetric with a tendency to the left.

Table 2 summarizes the obtained results of this study.

Table 2. Maximum safe rotation speed and skewness of the distribution for threshold of stability for each considered disc mass

Disc Mass [kg]	Maximum safe rotation speed [rad/s]	Skewness	Instability zone [rad/s]
10	700	-0.0266	780-850
100	780	0.6015	795-940
200	950	0.4740	950-1360
300	1200	0.3518	1180-1840

4. CONCLUSION

This paper analyzed the influence of uncertainties on the fluid induced instability on rigid rotors. The parameters subjected to uncertainties were the bearing clearance, the oil viscosity, the bearing radius and the bearing length.

The results show that, as expected, the mentioned uncertainties may introduce a failure in an angular velocity smaller than the expected without considering this uncertainties. For a "light" rotor, the threshold varies less and the skewness of the *pdf* is negative. For a "heavy" rotor, the threshold varies more and the skewness of the *pdf* is positive, but for a heavier rotor the skewness tend to be smaller.

5. ACKNOWLEDGEMENTS

The authors thank CAPES for providing financial support for this work. Acknowledgments are also extended to grant #2015/ 20363-6, São Paulo Research Foundation (FAPESP) and LAMAR/UNICAMP.

6. REFERENCES

Bently, D. E., 2001. "The Death of Whirl and Whip". *Orbit*. Fourth quarter, pp. 42-46.

Didier J., Sinou J-J. Faverjon B., 2012. "Study of the non-linear dynamic response of a rotor system with faults and uncertainties", *Journal of Sound and Vibration*, 331, pp-671-703

Krämer, E., 1993, *Dynamics of Rotors and Foundations*, Springer-Verlag, Berlin, 1st edition.

Machado T. H., Cavalca K. L., 2015. "Modeling of hydrodynamic bearing wear in rotor-bearing systems", *Mechanics Research Communications*, vol. 69, pp 15-23

Newkirk, B. L., and Taylor, H. D, 1925. "Shaft Whipping due to Oil Action in Journal Bearings", *General Electric Review*, Vol. 28, n. 8, 1925, pp. 559-568.

Ocvirk, E W., 1952. "Short bearing approximation for full journal bearings", *National Advisory Committee for. Aeronautics*, Technical Note 2808, Cornell University.

Sampaio, R. and Lima, R.Q., 2012. "Modelagem Estocástica e Geração de Amostras de Variáveis e Vetores Aleatórios" *SBMAC*, São Carlos.

7. RESPONSIBILITY NOTICE

The authors are the only responsible for the printed material included in this paper.